Communication: Uncovering correlated vibrational cooling and electron transfer dynamics with multidimensional spectroscopy

Zhenkun Guo, Paul G. Giokas, Thomas P. Cheshire, Olivia F. Williams, David J. Dirkes, Wei You, and Andrew M. Moran[a)]
Department of Chemistry, University of North Carolina at Chapel Hill, Chapel Hill, North Carolina 27599, USA

(Received 5 August 2016; accepted 30 August 2016; published online 14 September 2016)

Analogues of 2D photon echo methods in which two population times are sampled have recently been used to expose heterogeneity in chemical kinetics. In this work, the two population times sampled for a transition metal complex are transformed into a 2D rate spectrum using the maximum entropy method. The 2D rate spectrum suggests heterogeneity in the vibrational cooling (VC) rate within the ensemble. In addition, a cross peak associated with VC and back electron transfer (BET) dynamics reveals correlation between the two processes. We hypothesize that an increase in the strength of solute-solvent interactions, which accelerates VC, drives the system toward the activationless regime of BET. *Published by AIP Publishing.* [http://dx.doi.org/10.1063/1.4962670]

Multidimensional laser spectroscopies have emerged as indispensable tools with broad applicability in the past 15-20 yr.[1–8] Most multidimensional spectroscopies reveal correlations between vibrational and/or electronic resonances with pulse sequences related to the photon echo technique.[3,6,7] For example, two-dimensional (2D) electronic spectroscopies have been used to investigate processes ranging from energy transfer in photosynthetic proteins[9–11] to correlations between excitons in quantum wells.[12,13] Such photon echo spectroscopies are capable of uncovering heterogeneity in the resonance frequencies within an ensemble but cannot resolve the distribution of incoherent relaxation rates in the "waiting time" between excitation and detection (i.e., the "population time"). Berg and co-workers addressed this limitation by developing a fifth-order experiment, referred to as multiple population-period transient spectroscopy (MUPPETS), in which correlations between incoherent processes are exposed by scanning two population times.[14–20] Two-dimensional inverse-Laplace transformation of the MUPPETS signal with respect to the two population times reveals heterogeneity in the relaxation processes that take place in each delay time.[14,15,18] This versatile approach has been used to investigate photophysics in semiconductors[16,19] and various aspects of ionic liquids.[17,20]

In this communication, we use a two-color version of the MUPPETS technique to investigate correlations between vibrational cooling and electron transfer dynamics in a transition metal complex composed of titanium and catechol, $[Ti(cat)_3]^{2-}$ (see inset in Figure 1). This work builds upon our earlier investigation of this system, which employed traditional transient absorption spectroscopy.[21] Strong ligand-metal interactions in $[Ti(cat)_3]^{2-}$ give rise to a charge transfer electronic resonance near 400 nm. Photoexcitation of the charge transfer resonance induces quasi-instantaneous electron transfer from the ligands to titanium, whereas the subsequent back electron transfer (BET) process from titanium to the ligands takes place on the 180-fs time scale.[21,22] Correlation between the strength of the solute-solvent interactions, which is reflected by the vibrational cooling (VC) rate, and the time-scale of the BET process is of primary interest in this work. Traditional transient absorption spectroscopy cannot provide this information because it possesses only one population time. However, the MUPPETS technique can be used to expose correlations between the VC and BET processes.

Two-color MUPPETS experiments are conducted using the "pump-repump-probe" experimental setup described in Ref. 23. It should be noted that our three-beam geometry differs from the six-beam geometry of Berg and co-workers; however, the fifth-order nonlinearity of interest is the same.[18] The present experiment isolates the MUPPETS response by chopping the first two pulses that arrive at the sample, whereas the six-beam geometry of Berg and co-workers induces signal emission in a background-free direction. The first two pulses are centered at 408 nm and have 17-fs duration. The third pulse is a continuum generated in a sapphire window and is relayed to the sample with reflective optics. The four conditions needed to isolate the MUPPETS response are produced with two chopper wheels that are operated at 250 Hz and have relative phases that are shifted by 90°. Signal detection is accomplished with a CMOS array detector that is synchronized to the 1-kHz repetition rate of the laser system. The signals are averaged for 20 scans of the delay lines from 0 to 4 ps. Synthesis of $[Ti(cat)_3]^{2-}$ is carried out using the procedure described in Ref. 24. The aqueous solutions are flowed through a wire-guided jet with a thickness of 300 μm during experiments. The absorbance of the solution is equal to 0.5 at 408 nm in the 300-μm path length.

General aspects of the pulse sequence and approach for signal interpretation are summarized in Figure 1. The experiment begins when the first 408-nm pulse induces

a)Author to whom correspondence should be addressed. Electronic mail: ammoran@email.unc.edu

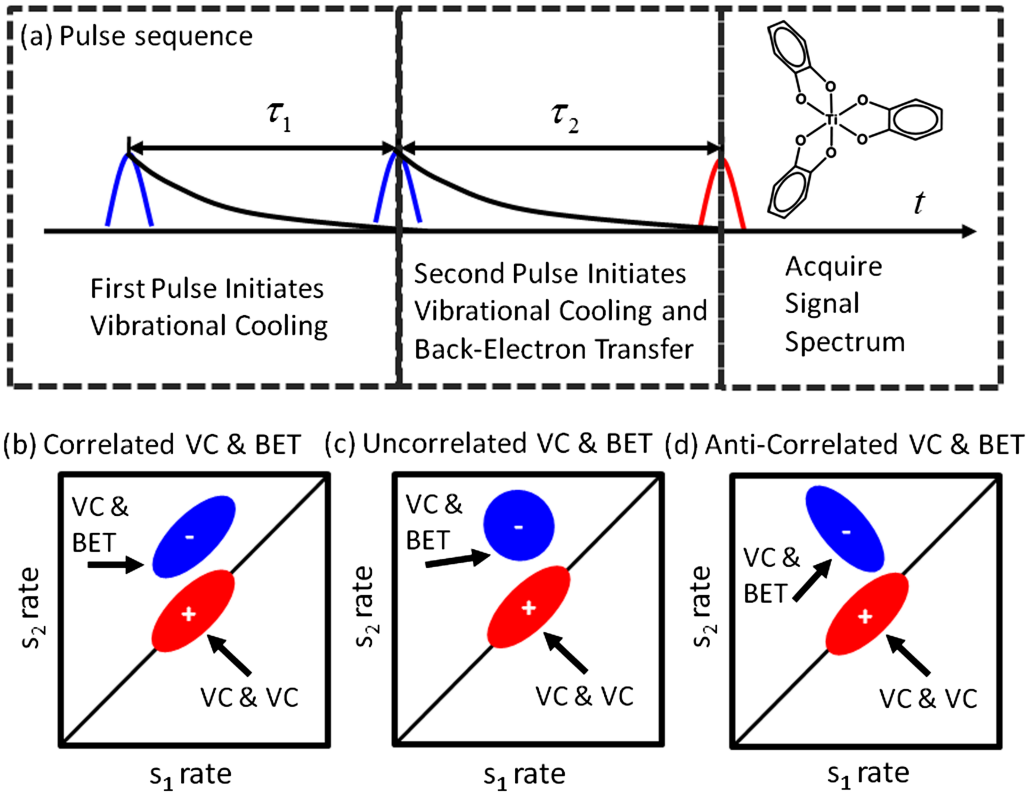

FIG. 1. (a) The first two pulses are centered at 408 nm, whereas the third pulse is a broadband continuum. The signal is primarily sensitive to vibrational cooling in τ_1 but carries signatures of both vibrational cooling and back-electron transfer in τ_2 because of the red-shifted probe wavelength. Transformation of the signal into a 2D rate spectrum reveals correlations between the dynamics in the two delay times. The diagonal peak associated with vibrational cooling has a correlated line shape because of heterogeneity in the ensemble. The cross peak between vibrational cooling and back-electron transfer processes may reveal (b) correlated, (c) uncorrelated, or (d) anti-correlated dynamics.

electron transfer from the ligands to titanium. Light absorption and electron transfer are one in the same process in this system because a charge transfer resonance is excited.[21,22] Photoexcitation of the charge transfer resonance with a second 408-nm pulse ensures that the signal is primarily sensitive to VC in the first delay time. That is, the response associated with the ground state relaxes on the time scale of VC. The information associated with the second delay time, τ_2, depends on the detection wavelength. Sensitivity to the BET process is achieved at probe wavelengths longer than 400 nm because the "hot" ground state produced by BET is red-shifted from the equilibrium absorbance spectrum.[21,22] Transient absorption signals are sensitive to both BET and VC dynamics throughout the visible signal spectrum; however, we find that the two components have similar magnitudes at a detection wavelength of 450 nm. Components with similar magnitudes are desired to expose correlations between the VC and BET processes through the 2D rate spectrum.[15] Data analysis is also facilitated by signal detection at 450 nm because of (i) the fairly large signal strength in this region of the spectrum and (ii) the absence of contributions from species with long-lived excited states at longer wavelengths.[21]

In Figure 2, we present MUPPETS signals and illustrate the microscopic dynamics of interest. Photoexcitation of the charge transfer resonance initiates both VC and BET dynamics. The excited state wavepacket does not traverse the point of degeneracy in the solvation coordinate because the system is deep within the inverted regime (see Figure 2(a)). Therefore, intramolecular Franck-Condon active modes must promote the ultrafast BET transition across the large free energy gap.[21] The signals presented in Figure 2(c) reveal a resonance associated with the hot ground state produced by BET at wavelengths longer than 470 nm. We note that the sign of the signal ($\Delta\Delta A$) is opposite to that measured with a traditional transition absorption experiment (ΔA) in the same wavelength region (i.e., the sign switches when the order of the nonlinearity changes by 2). The response at wavelengths shorter than 470 nm possesses contributions from VC dynamics in the ground electronic state. Contributions from excited state solvation are negligible because of the ultrafast time scale of the BET process. We do not observe signatures of stimulated emission with our 60-fs time resolution.

Previous work has demonstrated that 2D rate spectra are capable of revealing new insights into chemical processes; [14–20] however, this type of analysis can be challenging in practice because a 2D inverse-Laplace transform cannot be carried out on experimental data. In Figures 2(d)-2(f), the maximum entropy method (MEM) is used to fit experimental MUPPETS data and obtain rate distributions associated with the two dimensions. The data are fit to a linear combination of 2601 exponential functions using the Newton-Raphson method (i.e., products of 51 exponential functions for each dimension). Time constants of the exponentials range from 10 fs to 100 ps in logarithmic steps. The MEM algorithm is

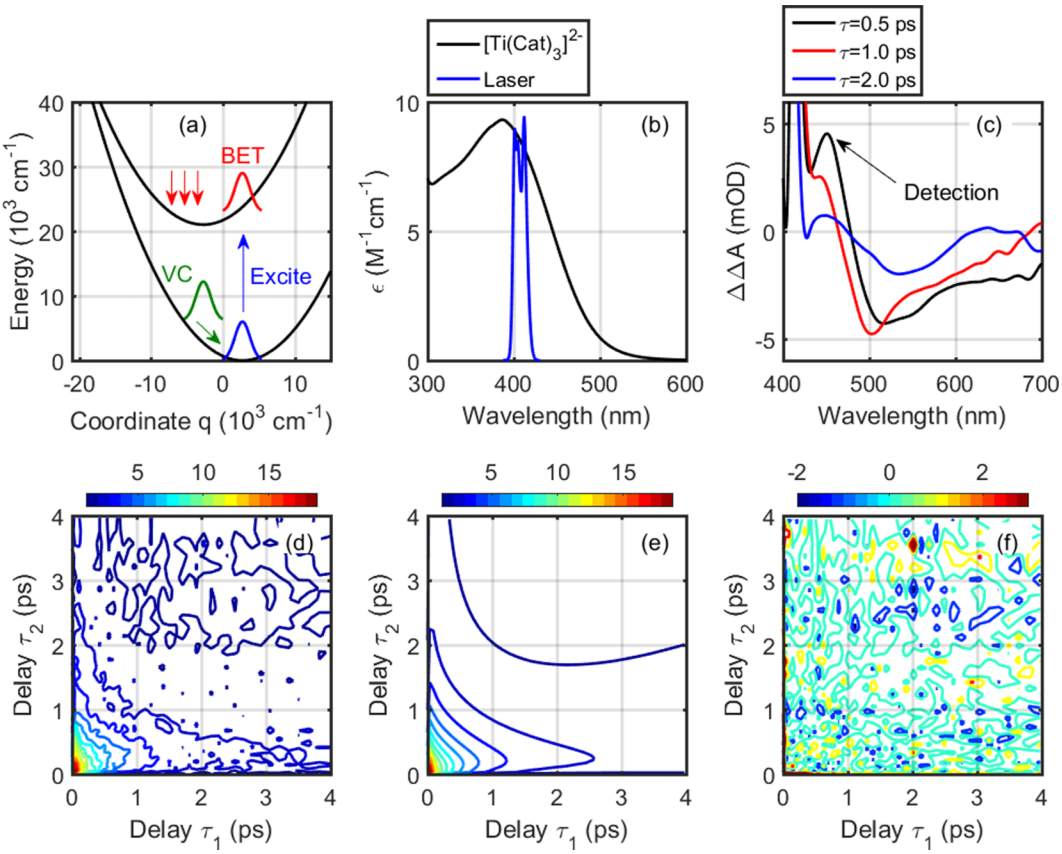

FIG. 2. (a) Physical picture of excited state dynamics in the solvation coordinate. Photoexcitation is followed by ultrafast back-electron transfer (BET). After BET, the wavepacket in the "hot ground state" undergoes a vibrational cooling (VC) process. (b) The system is excited near the maximum of the charge-transfer band. (c) At a detection wavelength of 450 nm, the MUPPETS signals carry information about BET and VC dynamics. Delay times in the legend represent the diagonal of the signal ($\tau = \tau_1 = \tau_2$). The (d) MUPPETS signal at 450 nm is (e) fit using the maximum entropy method. Residuals for the fit are shown in panel (f).

constrained to produce the smallest number of peaks that is consistent with the experimental data.[25] Thus, heterogeneity in a single relaxation process induces line broadening in the rate domain, whereas contributions from multiple processes with different rates give rise to separate peaks. The primary strength of the MEM approach is that it produces 2D rate spectra without assumptions about the physical processes that affect the spectroscopic signals. Details related to our MEM implementation and numerical tests for stability are discussed in the supplementary material.

In Figure 3, we present the two-dimensional MEM correlation spectrum associated with the fit in Figure 2. As suggested in Figure 1, the peak with the correlated line shape on the diagonal of the spectrum provides information about heterogeneity in the VC rate, whereas the "cross peak" above the diagonal represents VC in s_1 and BET in s_2. The cross peak has an opposite sign to the peak on the diagonal because BET causes the signal magnitude to rise and VC causes it to decay.[26] Nonetheless, the two signal components can be decomposed with the MEM analysis presented here (see the supplementary material for details) or by fitting traditional transient absorption data (see Ref. 21). The diagonal and cross peaks are centered near 3 and 1 ps^{-1} on the s_1 axis, respectively. It is possible that interference between signal components with different signs is responsible for the shift between peaks along the s_1 axis (in which case the shift does not communicate interesting physical information). In an alternate interpretation of the difference in peak positions, the members of the ensemble that undergo the slowest VC processes in τ_1 (i.e., rate constants near 1 ps^{-1}) are most likely to exhibit BET after photoexcitation by the second pulse. Such an interpretation cannot be justified based purely on energetic arguments under the non-adiabatic approximation; however, solvent dynamics may affect BET when adiabatic effects take hold.[27–30]

In Figure 3, line shapes in the 2D rate spectrum are analyzed using a linear regression algorithm in which points are weighted by the signal intensity; the slopes are computed with respect to logarithms of the two variables, $\log(s_1)$ and $\log(s_2)$. The positive sign of the slope for the peak on the diagonal signifies variation of the VC rate within the ensemble, whereas the positive sign of the slope for the peak above the diagonal suggests correlation between the VC and BET rates. That is, the orientation of the cross peak suggests that members of the ensemble which undergo fast VC dynamics tend to exhibit the fastest BET rates. The slope of 0.41 detected for the diagonal peak is smaller than the theoretically predicted slope of 1.0.[31] We hypothesize that this discrepancy between experiment and theory may arise when the VC dynamics in τ_2 are affected by the transfer of vibrational energy into the solvent during τ_1 (i.e., the processes in τ_1 and τ_2 are not equivalent because of the

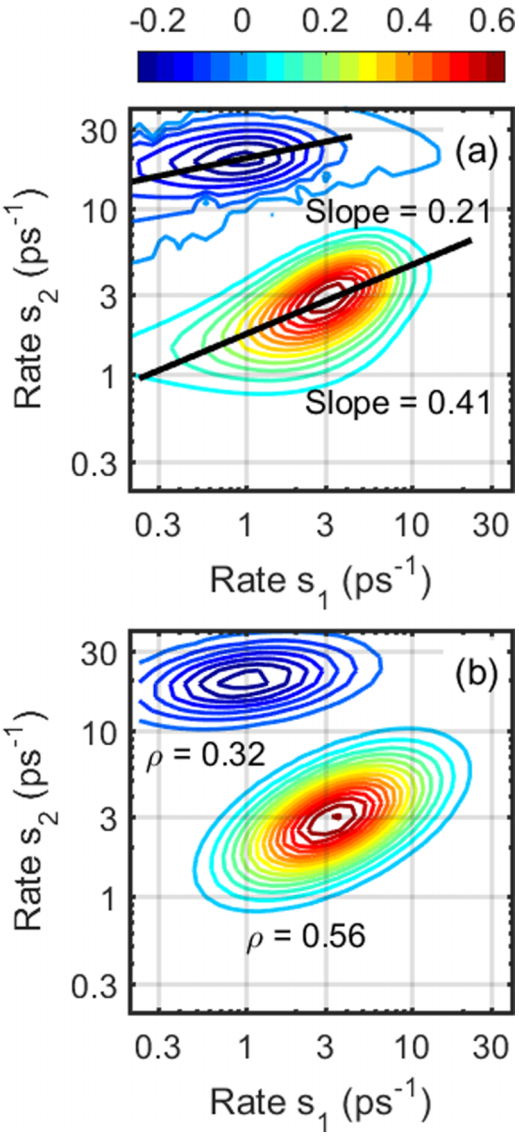

FIG. 3. (a) Two-dimensional MEM rate distribution obtained at a detection wavelength of 450 nm. The dimensions, s_1 and s_2, are conjugate to the delay times, τ_1 and τ_2. The positive sign of the slope for the diagonal peak is a signature of heterogeneity in the VC rate within the ensemble. The positive sign of the slope for the cross peak above the diagonal suggests that the VC and BET rates are correlated. The slopes are computed with respect to logarithms of the rates, $\log(s_1)$ and $\log(s_2)$. (b) The rate spectrum is fit to a sum of two Gaussian functions with correlation parameters, ρ, that interpolate between the homogeneous ($\rho = 0$) and inhomogeneous ($\rho \pm 1$) limits ($\rho < 0$ is possible for cross peaks).

nonequilibrium state of the solvent in τ_2). Another possibility is that the slope of the diagonal peak is less than 1.0 because of interference between signal components associated with the VC and BET processes. Such interference is a likely prospect because it would also explain why the peaks are shifted on the s_1 axis. We have also fit the rate spectrum to a sum of two Gaussian functions to account for interference. The correlation parameters for the Gaussian functions, ρ, interpolate between the homogeneous ($\rho = 0$) and inhomogeneous ($\rho = \pm 1$) limits ($\rho < 0$ is possible for cross peaks). This method of fitting also indicates heterogeneity in the rate of VC and correlation between VC and BET. Details associated with the Gaussian fit are described in the supplementary material.

The line shape of the cross peak suggests that a common physical parameter affects both VC and BET processes. The origin of such correlated dynamics can be considered in the context of the second-order rate formulas. The rate of VC can be expressed as the time integral of a time-correlation function in the solute-solvent interaction potential[32]

$$k_{VC} = \frac{1}{\hbar^2} \int_0^\infty dt \left\langle \hat{V}(t)\, \hat{V}(0) \right\rangle, \tag{1}$$

where $\hat{V}$ represents a combination of interactions (e.g., Coulombic, van der Waals, etc). Because of its ultrafast time scale, the BET process is most rigorously described with a nonequilibrium model that incorporates nuclear relaxation;[21] however, the basic physics can be understood in the framework of the equilibrium equation for electron transfer[33]

$$k_{BET} = \frac{2\pi |H_{DA}|^2}{\hbar \sqrt{4\pi \lambda k_B T}} \exp\left[-\frac{(\Delta G + \lambda)^2}{4 \lambda k_B T} \right]. \tag{2}$$

The free energy gap, ΔG, and reorganization energy, λ, are expected to be sensitive to the magnitude of the solute-solvent interaction potential, $\hat{V}$. Although the adiabaticity of the BET process may not be negligible, the overlap of the wavepacket with the region of the avoided crossing should be small because the system is deep within the inverted regime (see Figure 2(a)). Therefore, we suggest that the adiabaticity of the process corresponds to an intermediate regime, where the rate of the BET process can be approximated with Equation (2).[29,30,34]

In solvatochromic theory, ΔG should decrease as the strength of the solute-solvent interactions increases in a polar solvent.[35] Conversely, the solvent reorganization energy, λ, should increase with the strength of solvation; for example, the Stokes shift is equal to 2λ in the limit that the solvent induces solute fluctuations with Gaussian statistics.[36] Thus, an increase in the solute-solvent interaction potential, $\hat{V}$, can be anticipated to move the BET process, which is deep within the inverted regime, closer to the activationless regime (i.e., smaller $|\Delta G|$ and larger λ). In other words, the BET rate should be fastest for the subset of molecules that undergo the most rapid VC dynamics (i.e., the subset of molecules with largest $\hat{V}$). It is instructive to consider that even fairly minor differences in solvation environments can have a significant impact on the rate of BET. For example, the parameters, ΔG and λ, determined in our earlier work are −20 100 and 3290 cm^{-1}, respectively.[21] Increasing both ΔG and λ by 100 cm^{-1} increases the rate constant, k_{BET}, by a factor of 275. The description of BET becomes far more complicated when nonequilibrium effects are taken into account. Nonetheless, the present discussion establishes plausible connections between the VC and BET rates which are consistent with the line shape of the cross peak.

In summary, we have obtained a 2D rate spectrum for the transition metal complex, $[Ti(cat)_3]$,[2] by combining two-color MUPPETS signals and the MEM numerical method. The correlated line shape of the diagonal peak in the 2D spectrum reflects a heterogeneous distribution of VC rates within the ensemble. The line shape of the cross peak suggests correlation between VC and BET processes. We hypothesize

that an increase in the solute-solvent interaction potential, which affects the rate of VC, drives the BET process toward the activationless regime, thereby accelerating the rate of BET.

See supplementary material for a detailed description of our implementation of the maximum entropy method. Details associated with the Gaussian fit in Figure 3 are also described.

This work was primarily funded by the UNC Energy Frontier Research Center (EFRC) "Center for Solar Fuels," an EFRC funded by the U.S. Department of Energy, Office of Science, Office of Basic Energy Sciences under Award No. DE-SC0001011 (T.P.C., P.G.G., and Z.G.). EFRC support was used to conduct spectroscopic experiments and develop the theoretical model. W.Y. and D.J.D. synthesized $[Ti(cat)_3]^{2-}$ with support from the Office of Naval Research (Grant No. N000141410221).

[1]O. Golonzka, M. Khalil, N. Demirdöven, and A. Tokmakoff, Phys. Rev. Lett. **86**, 2154–2157 (2000).
[2]M. C. Asplund, M. T. Zanni, and R. M. Hochstrasser, Proc. Natl. Acad. Sci. U. S. A. **97**, 8219–8224 (2000).
[3]D. M. Jonas, Annu. Rev. Phys. Chem. **54**, 425–463 (2003).
[4]T. Brixner, T. Mancal, I. V. Stiopkin, and G. R. Fleming, J. Chem. Phys. **121**, 4221–4236 (2004).
[5]M. L. Cowan, J. P. Ogilvie, and R. J. D. Miller, Chem. Phys. Lett. **386**, 184–189 (2004).
[6]J. P. Ogilvie and K. J. Kubarych, Adv. At., Mol., Opt. Phys. **57**, 249–321 (2009).
[7]P. Hamm and M. T. Zanni, *Concepts and Methods of 2D Infrared Spectroscopy* (Cambridge University Press, Cambridge, 2011).
[8]J. C. Wright, Annu. Rev. Phys. Chem. **62**, 209–230 (2011).
[9]G. S. Schlau-Cohen, A. Ishizaki, and G. R. Fleming, Chem. Phys. **386**, 1–22 (2011).
[10]K. L. M. Lewis and J. P. Ogilvie, J. Phys. Chem. Lett. **3**, 503–510 (2012).
[11]A. Chenu and G. D. Scholes, Annu. Rev. Phys. Chem. **66**, 69–96 (2015).
[12]K. W. Stone, D. B. Turner, K. Gundogdu, S. T. Cundiff, and K. A. Nelson, Acc. Chem. Res. **42**, 1452–1461 (2009).
[13]L. Yang, I. V. Schweigert, S. T. Cundiff, and S. Mukamel, Phys. Rev. B **75**, 125302 (2007).
[14]E. van Veldhoven, C. Khurmi, X. Zhang, and M. A. Berg, ChemPhysChem **8**, 1761–1765 (2007).
[15]C. Khurmi and M. A. Berg, J. Chem. Phys. **129**, 064504 (2008).
[16]S. J. Kern, S. Kalyanasis, and M. A. Berg, Nano Lett. **11**, 3493–3498 (2011).
[17]K. Sahu, S. J. Kern, and M. A. Berg, J. Phys. Chem. A **115**, 7984–7993 (2011).
[18]M. A. Berg, Adv. Chem. Phys. **150**, 1–102 (2012).
[19]K. Sahu, H. Wu, and M. A. Berg, J. Am. Chem. Soc. **135**, 1002–1005 (2013).
[20]S. D. Verma, S. A. Corcelli, and M. A. Berg, J. Phys. Chem. Lett. **7**, 504–508 (2016).
[21]Z. Guo, P. G. Giokas, T. P. Cheshire, O. F. Williams, D. J. Dirkes, W. You, and A. M. Moran, J. Phys. Chem. A **120**, 5773–5790 (2016).
[22]Y. Wang, K. Hang, N. A. Anderson, and T. Lian, J. Phys. Chem. B **107**, 9434–9440 (2003).
[23]Z. Guo, B. P. Molesky, T. P. Cheshire, and A. M. Moran, J. Chem. Phys. **143**, 124202 (2015).
[24]B. A. Borgias, S. R. Cooper, Y. B. Koh, and K. N. Raymond, Inorg. Chem. **23**, 1009–1016 (1984).
[25]A. T. N. Kumar, L. Zhu, J. F. Christian, A. Demidov, and P. M. Champion, J. Phys. Chem. B **105**, 7847–7856 (2001).
[26]P. G. Giokas, "Investigating Molecule-Semiconductor Interfaces with Nonlinear Spectroscopies," Ph.D. thesis (University of North Carolina, 2016).
[27]L. D. Zusman, Chem. Phys. **49**, 295–304 (1980).
[28]H. Sumi and R. A. Marcus, J. Chem. Phys. **84**, 4894–4914 (1985).
[29]Y. J. Yan, M. Sparpaglione, and S. Mukamel, J. Phys. Chem. **92**, 4842–4853 (1988).
[30]A. A. Stuchebrukov and X. Song, J. Chem. Phys. **101**, 9354–9365 (1994).
[31]M. A. Berg and J. R. Darvin, J. Chem. Phys. **145**, 054119 (2016).
[32]J. C. Owrutsky, D. Raftery, and R. M. Hochstrasser, Annu. Rev. Phys. Chem. **45**, 519–555 (1994).
[33]P. F. Barbara, T. J. Meyer, and M. A. Ratner, J. Phys. Chem. **100**, 13148–13168 (1996).
[34]H. Sumi, J. Phys. Soc. Jpn. **49**, 1701–1712 (1980).
[35]C. Reichardt and T. Welton, *Solvents and Solvent Effects in Organic Chemistry*, 4th ed. (Wiley-VCH, Weinheim, 2011).
[36]S. Mukamel, *Principles of Nonlinear Optical Spectroscopy* (Oxford University Press, New York, 1995).